# 4-Hydroxy-2(E)-nonenal Metabolism Differs in Apc^{+/+} Cells and in Apc[Min/+] Cells: It May Explain Colon Cancer Promotion by Heme Iron

Maryse Baradat, Isabelle Jouanin, Sabine Dalleau, Sylviane Taché, Mathilde Gieules, Laurent Debrauwer, Cécile Canlet, Laurence Huc, Jacques Dupuy, Fabrice H. F. Pierre, and Françoise Guéraud*

INRA UMR1331, TOXALIM (Research Center in Food Toxicology), Université de Toulouse, ENVT, INP, UPS, ToxAlim, 180 chemin de Tournefeuille, F-31027 Toulouse, France

ABSTRACT: Animal and epidemiological studies suggest that dietary heme iron would promote colorectal cancer. Oxidative properties of heme could lead to the formation of cytotoxic and genotoxic secondary lipid oxidation products, such as 4-hydroxy-2(E)-nonenal (HNE). This compound is more cytotoxic to mouse wild-type colon cells than to isogenic cells with a mutation on the adenomatous polyposis coli (APC) gene. The latter thus have a selective advantage, possibly leading to cancer promotion. This mutation is an early and frequent event in human colorectal cancer. To explain this difference, the HNE biotransformation capacities of the two cell types have been studied using radiolabeled and stable isotope-labeled HNE. Apc-mutated cells showed better biotransformation capacities than nonmutated cells did. Thiol compound conjugation capacities were higher for mutated cells, with an important advantage for the extracellular conjugation to cysteine. Both cells types were able to reduce HNE to 4-hydroxynonanal, a biotransformation pathway that has not been reported for other intestinal cells. Mutated cells showed higher capacities to oxidize 4-hydroxynonanal into 4-hydroxynonanoic acid. The mRNA expression of different enzymes involved in HNE metabolism such as aldehyde dehydrogenase 1A1, 2 and 3A1, glutathione transferase A4—4, or cystine transporter xCT was upregulated in mutated cells compared with wild-type cells. In conclusion, this study suggests that Apc-mutated cells are more efficient than wild-type cells in metabolizing HNE into thiol conjugates and 4-hydroxynonanoic acid due to the higher expression of key biotransformation enzymes. These differential biotransformation capacities would explain the differences of susceptibility between normal and Apc-mutated cells regarding secondary lipid oxidation products.
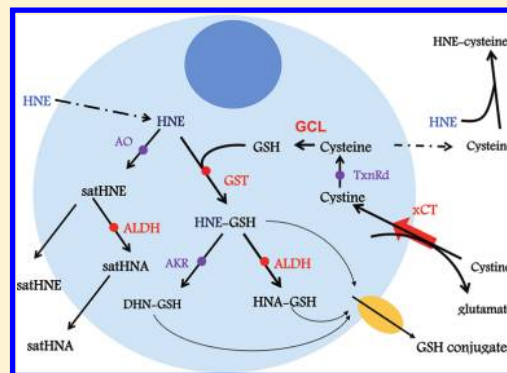
■ INTRODUCTION

Colorectal cancer (CRC) is the first cause of death by cancer in nonsmokers in affluent countries. Environmental factors such as food are believed to play a role in the development of CRC, as promoting or preventing agents. The intake of heme iron rich food, such as red or processed meat, is associated with an elevated risk of CRC.[1−3] On the basis of meta-analyses of epidemiological studies, the World Cancer Research Fund panel (WCRF) in its 2007 report considers as convincing the risk associated with red and processed meat and recommends limiting red meat and avoiding processed meat consumption.[4] In contrast, fish and white meat intake is not associated with an increase of CRC risk. As heme iron concentration is much higher in red meat than in white meat, it might be involved in the promoting effect of red meat. Indeed, we previously reported that dietary heme, in the form of either hemoglobin, hemin, red and processed meat, promotes the growth of precancerous lesions, aberrant crypt foci (ACF), and mucin depleted foci in the colon of rats given a low-calcium diet.[5−8] The mechanisms underlying these observations are not known. It could be related to the pro-oxidative properties of heme iron, which induces the oxidation of dietary polyunsaturated fatty acids present in the diet. This oxidation gives rise to reactive secondary lipid oxidation product formation, such as malondialdehyde and hydroxyalkenals. We and other authors have evidenced dietary heme-induced effects such as lipid peroxidation, increased proliferation, and genotoxicity.[5,6,9,10]

Several secondary lipoperoxidation products have been characterized, especially concerning their biological roles. They can be found as food contaminants and are also endogenously formed under basal conditions, and their production increases under oxidative stress conditions. These reactive endogenous aldehydes are thus considered as "second messengers" of oxidative stress.[11,12] The same aldehydes are present in the diet, particularly in heme-iron and polyunsaturated fat rich food,[13] and probably also formed during digestion. They are cytotoxic and genotoxic. 4-Hydroxy-2(E)-nonenal (HNE) is one of the major alkenals formed upon linoleic and arachidonic acid oxidation and can play a role in the regulation of cell cycle.[14]

In a previous work, we have compared the effect of HNE treatment in immortalized mouse colonic epithelial normal cells (Apc^{+/+}) and in mouse colonic epithelial preneoplastic cells

(Apc[Min/+]).[15] Those cells deriving from wild type and Min mice crossed with Immortomouse mice represent an interesting *in vitro* model to investigate the mechanisms by which dietary components may impact colon cancer promotion and progression. Min mice, that are genetically predisposed to develop intestinal tumors, bear a mutation on the *Apc* gene, and loss of Apc function is known to be a frequent and early event in human CRC development. We have shown that HNE is more cytotoxic to normal cells than to preneoplastic cells at the same concentration.[15] We thus suggest that HNE would promote colorectal carcinogenesis by selecting surviving mutated cells, as observed previously in rats with cholic acid.[16]

The aim of the present study was to evaluate the involvement of HNE metabolism in the differential cytotoxic effect in immortalized colonic epithelial mouse cell lines, mutated or not on the *Apc* gene. For this purpose, we have used HNE labeled with both radioactive (^{3}H) and stable (^{13}C) isotopes to get an accurate determination of HNE biotransformations. We report here a differential HNE biotransformation pathway regulation in both cell lines. In Apc-mutated cells, we showed higher HNE-thiol conjugates and 4-hydroxynonanoic acid levels due to the higher expression of key biotransformation enzymes. These differential biotransformation capacities would explain the differences of susceptibility in normal and preneoplastic cells regarding secondary lipid oxidation products.

■ EXPERIMENTAL PROCEDURES

Chemicals. γ-Nonalactone, ethyl 2-bromoacetate, and BHT were purchased from Aldrich (France). Solvents, 4-chlorothiophenol, hydrogen peroxide (30% in water), *n*-heptanal, and DIBAL (1 M in *n*-hexane) were purchased from Acrös Organics (Belgium). *N*-Heptanal was distilled before use. Ethyl [1,2-[13]C$_2$]-2-bromoacetate (99% atom ^{13}C) was purchased from Eurisotop (France). PBS and L-cystine hydrochloride were purchased from Sigma (France). DMEM was purchased from Gibco (Invitrogen, France).

[1,2-[13]C$_2$]-4-Hydroxy-2(E)-nonenal (^{13}C-HNE). ^{13}C-HNE was prepared according to our published method,[17] with modifications. Ethyl [1,2-[13]C$_2$]-2-bromoacetate was converted to ethyl 4-hydroxy-2(E)-nonenoate by reacting consecutively with 4-chlorothiophenol, hydrogen peroxide, and *n*-heptanal as described.[18] The remaining steps were unchanged, and the overall yield was improved to 20%.

4-Hydroxy-2(E)-nonenal (HNE). HNE was prepared from ethyl 2-bromoacetate by the same method as that for ^{13}C-HNE.

Mixtures containing 2/3 molar amounts of HNE/^{13}C-HNE were prepared for cell experimentation and were checked by NMR (^{1}H, CDCl$_3$).

4-Hydroxynonanal Hemiacetal (Saturated HNE (satHNE)). γ-Nonalactone was reduced to satHNE by DIBAL as described,[19] with slight modifications. Briefly, 30 mL of DIBAL was added dropwise (1 h) to a cooled solution (−50 °C) of γ-nonalactone (3 mL) in 200 mL of petroleum ether (40−60 °C boiling range). After stirring for 1 h at −35 °C, methanol (10 mL), water (0.5 mL), silica, and magnesium sulfate were added. BHT was added to the crude mixture which was filtered and washed once with water. The satHNE sample was purified by preparative TLC (silica gel; elution with *n*-hexane/DCM/MeOH 70/30/2). Extraction with DCM containing methanol (4%) yielded satHNE (two diastereomers). The pure sample was analyzed by ^{1}H NMR (CDCl$_3$). It was stable for 4 days at +4 °C in water as checked by NMR (D$_2$O).

^{1}H NMR (CDCl$_3$). Diastereoisomer A: 5.54 (1H, d, *J* = 4.2 Hz, OC*H*OH); 4.18 (1H, m, OC*H*).

Diastereoisomer B: 5.45 (1H, d, *J* = 4.4 Hz, OC*H*OH); 3.98 (1H, m, OC*H*).

Both diastereoisomers: 2.14−1.25 (12H); 0.88 (3H, t, *J* = 6.2 Hz).

4-Hydroxynonanoic Acid (Saturated HNA (satHNA)). satHNA was synthesized by basic hydrolysis (1 M NaOH) of γ-nonalactone (+70 °C, 2 h). The mixture was acidified to pH 3 with 1 M phosphoric acid, then extracted 3 times with ethyl acetate, dried with magnesium sulfate, and evaporated in vacuo. The sample purity was checked by ^{1}H NMR (D$_2$O) and was stable for 4 days at +4 °C in water.

[4-^{3}H]-4-Hydroxy-2(E)-nonenal (^{3}H-HNE). ^{3}H-HNE was synthesized as described in our published method.[20] The radiosynthesis of [4-^{3}H]-4-hydroxy-2(E)-nonenal diethylacetal (aldehyde-protected precursor) was carried out at CEA, Service des Molecules Marquees, CEN, Saclay, France. The radiochemical purity was determined by HPLC (after acid hydrolysis with 1 mM HCl) and was found to be 95%, while its specific activity was 222 GBq/mol.

Cell Culture and Treatment. Apc^{+/+} and Apc[Min/+] colon epithelial cells were established as described previously.[21,22] Cells harbor a temperature-sensitive mutation of the simian virus 40 (SV40) large tumor antigen gene (tsA58), under the control of interferon γ. All cells of these mice are immortalized; they express active SV40 at the permissive temperature (33 °C) and proliferate. Cells were seeded at a permissive temperature of 33 °C in 6 well culture plates with 2 mL of Dulbecco's modified essential medium (DMEM) supplemented with 10% fetal calf sera, 1% penicillin/streptomycin, 2% glutamine, and 10 U/ mL interferon γ. At subconfluence, i.e., 72 h after seeding, cells were placed for a 24-h period of adaptation at 37 °C without interferon γ to inhibit the SV40 transgene and limit proliferation, and without antibiotics. At nonpermissive temperatures, cell lines can be maintained in culture for 8 days, which is comparable with that of normal epithelial cells. Before experiments, cells were rinsed twice and preincubated for 15 min at 37 °C in 1 mL of DMEM without phenol red. [^{3}H]-HNE was added to 2/3 molar amount of HNE/^{13}C-HNE in water. Ten microliters of this solution was used for cell incubation. HNE concentration was checked spectrophotometrically (λ, 223 nm; ε, 13750 L mol⁻¹ cm⁻¹) before cell treatment.

At the end of the incubation time, culture supernatants were collected in tubes containing 50 μL of acetic acid and 10 μg of BHT, in order to stabilize metabolites. Cells were rinsed 3 times with cold PBS and added with 900 μL of 0.6 M perchloric acid in order to precipitate proteins. Precipitated cells were harvested and centrifuged for 5 min at 11600g. Supernatants were collected for further analysis. Precipitates were dissolved in 200 μL of 1 M NaOH and counted for radioactivity in a Packard 2200CA scintillation counter (Packard, PerkinElmer, France) using Packard Ultima Gold as the scintillation cocktail.

Some experiments were done under the same conditions but with phosphate buffered saline (PBS) solution instead of DMEM (see the Results section).

Some experiments were done by treating cells with 0.2 mM L-cystine in PBS for 30 min at 37 °C and incubating the resulting supernatant with 40 μM HNE for 30 min at 37 °C.

HPLC. HPLC analyses were carried out on a Kontron HPLC system (two Kontron 420 pumps (Kontron, Serlabo, France)) and the HPLC software Diamir (Agilent Technologies, France) equipped with a 100 μL loop for radio-HPLC HNE metabolic profiles or with a 500 μL loop for peak purification and connected to a Waters Spherisorb ODS2 column (5 μm, 4.6 × 250 mm) (Waters, France) in an oven set at 35 °C. This system was connected to an online radioactivity detector (Packard Flo-one Flow scintillation analyzer) using Flo-scint as the scintillation cocktail or connected to a Gilson FC 204 fraction collector (Gilson, France) and using Packard Ultima Gold as the scintillation cocktail and a Packard 2200CA as scintillation counter for peak purification. The separation of HNE metabolites was performed with 1 mL/min flow using two mobile phases. Mobile phase A contained water/acetonitrile/

acetic acid, 97.5/2.5/0.1; and mobile phase B contained water/aceto-nitrile/acetic acid, 40/60/0.1. The elution gradient was 0 min (15%B); 10 min (25%B); 20 min (26%B); and 40−50 min (65%B).

For the identification of the metabolite eluted at 41 min, culture supernatants were extracted by DCM, and the DCM phase was evaporated under vacuum. The dry extract was dissolved in 500 μL of HPLC mobile phase A and analyzed by HPLC. The peak at 41 min is collected and further purified using a 200 mg glass Chromabond SPE cartridge (Macherey-Nagel, France). The cartridge was eluted by $CDCl_3$ for further NMR analysis.

Mass Spectrometry Analyses. LC-MS: Cell culture supernatants were analyzed by LC-ESIMS using a Thermo Separation Products P1500 LC pump (Thermo Fisher, Les Ulis, France) fitted with the same column and using the same gradient elution as that described above (in the HPLC section). The flow rate was 1 mL/min with 1/5 post column splitting.

The liquid chromatograph was coupled to a Finnigan LCQ quadrupole ion trap mass spectrometer (Thermo Fisher) fitted with an electrospray ionization source operating in the negative mode. Typical ionization and ion transfer conditions were the following: electrospray needle, 4.5 kV; heated transfer capillary temperature, 220 °C; heated transfer capillary voltage, −20 V; and tube lens offset, 10 V. MS^2 experiments were carried out under automatic gain control using helium as the collision gas. Operating MS/MS ion excitation conditions (isolation width, excitation voltage, and excitation time) were adjusted to get maximum sensitivity and structural information for each compound of interest.

GC-MS: GC-MS analyses were achieved on a GC Trace (Thermo Electron, Les Ulis, France) gas chromatograph coupled to a Finnigan Polaris-Q ion trap mass spectrometer (Thermo Electron) by means of an AS2000 autosampler (Thermo Electron). The chromatographic separation was achieved on a BPX5 capillary column (25 m × 0.22 mm ID, 0.25 μm film thickness) from SGE (Courtaboeuf, France). Samples purified by fraction collection (typically 50−200 ng) were evaporated to dryness, resolved in a BSTFA/TMCS (99:1) mixture and heated at 60 °C during 1 h for trimethylsilylation. The resulting solution was then evaporated to dryness under a gentle stream of nitrogen and retaken in 100 μL of hexane for GC-MS analysis. Injections (1−2 μL) were made in the splitless mode. Helium was used as the carrier gas at a flow rate of 1 mL/min. The oven temperature was programmed as follows: 60 °C for 1 min, then 60 to 100 °C at 10 °C/min, 100 to 250 °C at 25 °C/min, and a final hold time of 13 min at 250 °C. The injector and GC-MS interface were set at 220 and 250 °C, respectively. Electron ionization mass spectra were acquired from m/z 50 to m/z 450 at a source temperature of 220 °C.

NMR Analysis. Peak 41 isolated by HPLC and the 4-hydroxynonanal hemiacetal synthesized were analyzed by NMR spectroscopy. NMR spectra were obtained at 300 K using a Bruker Avance DRX-600 spectrometer (Bruker, Karlsruhe, Germany) operating at 600.13 MHz and equipped with a 5 mm ^{1}H-^{13}C-^{15}N inverse triple resonance cryoprobe attached to a Cryoplatform (the preamplifier cooling unit). The sample isolated by HPLC and the synthesized standard were dissolved in 600 μL of deuterated chloroform ($CDCl_3$).

The one-dimensional spectrum was acquired using a standard pulse sequence for ^{1}H NMR; 2048 free induction decays (FIDs) were collected with a spectral width of 12 ppm into 32 K data points with a relaxation delay of 2 s and an acquisition time of 2.28 s. An exponential function equivalent to a line-broadening of 0.3 Hz was applied prior to Fourier transformation.

Quantitative RT-PCR. Cell RNA was isolated using TRI-RE-AGENT (Sigma, France) according to the manufacturer's instructions. Two-step Quantitative Reverse Transcriptase-PCR (RT-PCR) was performed using TBP (TATA Binding Protein) as the housekeeping gene. cDNA synthesis was obtained using the iScript cDNA Synthesis kit (Bio-Rad, France) with 1 μg of RNA. After reverse transcription, cDNA was amplified using iQ SYBR Green Supermix (Bio-Rad) by standard PCR with gene specific primers using a Bio-Rad CFX96 Real Time PCR detection system:

- xCT: (F)-5′ TGA AAT TCC TGA ACT TGC AAT CA 3′/ (R)-5′ TGA CAC TCG TGC TAT TTA GGA CCA T 3′
- AOR: (F)-5′ GAC AAA GCT GCC TGT AGA GTG G 3′/ (R)-5′ GCT GAC CAT CAC GGT TTC TCC A 3′
- GSTA4: (F)-5′ GAT GAT TGC CGT GGC TCC ATT TA 3′/ (R)-5′ CTG GTT GCC AAC GAG AAA AGC C 3′
- ALDH1A1: (F)-5′ GGA ATA CCG TGG TTG TCA AGC C 3′/ (R)-5′ CCA GGG ACA ATG TTT ACC ACG C 3′
- ALDH2: (F)-5′ GCT GTT GTA CCG ATT GGC GGA T 3′/(R)-5′ GCG GAG ACA TTT CAG GAC CAT G 3′
- ALDH3A1: (F)-5′ GGT CCT TGT CAT AGG TGC TTG G 3′/ (R)-5′ GAA AGC AGG TCT GCC ATG TGA TC 3′
- TBP: (F)-5′ ACT TCG TGC AAG AAA TGC TGA A 3′/ (R)-5′ GCA GTT GTC CGT GGC TCT CT 3′

Quantitative RT-PCR was conducted in a final reaction volume of 25 μL with 5 μL of cDNA, 7.5 μL of primers, and 12.5 μL of SYBR Green, using 0.2 mL of the thin wall PCR tube. Thermocycling conditions were set as follows: initial denaturation at 95 °C for 10 min, denaturation at 95 °C for 15 s, annealing at 60 °C for 30 s, and extension at 72 °C for 30 s.

Cytotoxicity Assay. Cells used for the cytotoxicity assay of HNE, satHNE, or satHNA were seeded into 96 well culture plates in DMEM culture medium. The cells were cultured at 33 °C with interferon γ until subconfluence and transferred at 37 °C without interferon γ for 24 h. After 24 h, cells were at confluence, and the culture medium was replaced with HNE, satHNE, or satHNA. Cells were incubated at 37 °C for 24 h. Cells were washed, then 100 μL of 3-(4,5-dimethyldiazol-2-yl)-2,5 diphenyl tetrazolium bromide solution (MTT/0.45 mg/mL in PBS) was added to each well, and the cells were incubated at 37 °C for 4 h. The reaction product was solubilized in 100 μL of lysis buffer (10% SDS and 0.01 M NaOH) before the color of the reaction product was quantified using a plate reader at 570 and 690 nm. The results are expressed in % of dead cells relative to untreated wells. These assays were performed in triplicate.

Statistical Analyses. ANOVA and Student's t test were done using GraphPad Prism software.

■ RESULTS

HNE Uptake. After 5 min of incubation with 40 μM HNE, the radioactivity in the cellular content of Apc$^{Min/+}$ cells was 3 times more important than in Apc$^{+/+}$ cells (10% vs 3% of dose), although the radioactivity linked to cellular proteins was the same (1%). After 30 min, there was still more radioactivity in the cellular content of Apc$^{Min/+}$ cells, but the radioactivity linked to proteins was lower in preneoplastic cells (1.7%) than in normal cells (2.6%).

Time and Concentration-Dependent Overall Metabolism of HNE. Cells were treated with different concentrations of HNE (5−40 μM) for 30 min or during different times (5−90 min) at 40 μM. For each time or concentration point of the experiments, preneoplastic cells showed a higher biotransformation capacity than normal cells did (Figure 1). At 20−40 μM/30 min HNE treatment, Apc$^{Min/+}$ cells metabolized 6 times more HNE than Apc$^{+/+}$ cells did. After a 30 min period of treatment, the percentage of unmetabolized HNE remained low for Apc$^{Min/+}$ cells (3 to 6%) and increased from 15% to 36% for Apc$^{+/+}$ cells, when increasing the treatment from 5 to 40 μM.

HPLC Profiles and Metabolite Identifications. Various peaks have been observed after incubations of both cell types
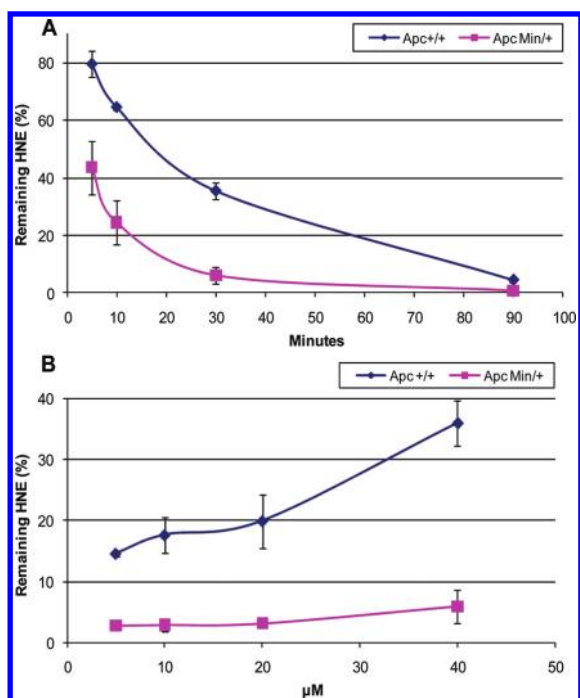
Figure 1. Time- and concentration-dependent metabolism of HNE. (A) For time-dependent studies, $Apc^{+/+}$ and $Apc^{Min/+}$ cells were treated with 40 μM HNE. (B) For concentration-dependent studies, $Apc^{+/+}$ and $Apc^{Min/+}$ cells were exposed during 30 min to various concentrations of HNE. Data are expressed as the mean of three separate experiments ± SD. All differences between $Apc^{+/+}$ and $Apc^{Min/+}$ cell lines are statistically significant (Student's t test) at $p < 0.01$.

after HNE treatment and radio-HPLC analyses of HNE metabolites (Figure 2). Minor peaks eluted at 3, 43, and 46 min were not further investigated since they were not quantitatively different between the two cell types.

As shown in Figure 2, a group of partially resolved peaks were eluted between 16 and 22 min. These retention times correspond to the isomers of the cysteine conjugate of HNE (HNE—cysteine) and to an unresolved mixture of the isomers of the glutathione conjugates of HNE (HNE-GSH) and its reduced form (DHN-GSH), respectively. Those conjugated metabolites were identified in a previous study on mouse colon epithelial cells (identical to $Apc^{+/+}$ cells) using mass spectrometry,[23] on the basis of diagnostic fragment ions corresponding to the cysteine (m/z 189) or glutathione (m/z 254 and m/z 272) moiety of the metabolites analyzed in the negative electrospray ionization mode. The peak eluted at Rt = 33 min (Peak 33) exhibited partially coeluting $[M - H]^-$ ions at m/z 171 and m/z 460. Additional MS/MS experiments on these three precursor ions showed the presence of a mixture of HNA (fragment ions at m/z 71, 127, and 153) and HNA-GSH in its lactone form (fragment ions at m/z 254, 272, 306, and 442), already identified in a previous study.[23] A third metabolite exhibited $[M - H]^-$ ions at m/z 173, yielding fragment ions at m/z 155, 127, and 129 in a subsequent MS/MS analysis. This metabolite was identified as satHNA, the oxidized and saturated derivative of HNE.

In addition to the metabolites whose identification was confirmed by LC-MS, some other peaks detected by radio-HPLC gave no response on the corresponding LC-MS chromatograms. This was the case in particular for the peak eluted at 31.7 min. (Figure 2). For this metabolite, GC-MS analysis was carried out after silylation of the collected radio-HPLC peaks. This peak

eluted at the same retention time as DHN. After silylation, GC-MS analysis did not show any DHN in this fraction but revealed the presence of a metabolite exhibiting characteristic ions at m/z 321 ($[M - CH_3]^+$), and fragment ions resulting from α-cleavages of the OH group in position 4, at m/z 173 and m/z 265, respectively. On the basis of this information, this metabolite was tentatively identified as a thiol derivative of DHN, a metabolite that had not been identified in HNE metabolism studies until now.

Finally, the peak at Rt = 41 min (Peak 41) could not be evidenced using negative electrospray LC-MS. Thus, this peak has also been isolated and further analyzed by positive electrospray ionization, which gave weak peaks at m/z 159 (MH^+) and m/z 141 ($MH - H_2O)^+$). The complete characterization of this metabolite was achieved by NMR. By comparison with literature data,[19] it corresponds to the saturated and cyclized form of HNE, 4-hydroxynonanal hemiacetal (saturated HNE; satHNE). Its identification was confirmed by comparison of its chemical shifts with those of a standard synthesized from γ-nonalactone (Figure 3). Apart from small peaks corresponding to BHT, solvent and small impurities in the synthesized standard, the chemical shifts matched with those of the isolated metabolite.

Metabolism Studies As a Function of Incubation Time and HNE Concentration. Table 1 shows the amount of the different metabolites as a function of incubation time and HNE concentration. In the present study, we have focused on metabolites or peaks that were quantitatively different between the two cells lines, as observed on radio-HPLC profiles (Figure 2). Those metabolites are HNE—cysteine (Rt = 16.5 min), satHNE (Rt = 41 min), peak at Rt = 33 min corresponding to a mixture of oxidized metabolites, as well as peaks eluted at Rt between 17.2 and 22 min corresponding to HNE and DHN glutathione conjugates.

HNE—cysteine formation was much higher for $Apc^{Min/+}$ cells than for $Apc^{+/+}$ cells, 13 nmol vs 2 nmol, respectively, after 30 min of incubation with 40 μM HNE. A large difference remained present whatever the concentration or the incubation duration. On the contrary, satHNE formation was much higher for $Apc^{+/+}$ cells than for $Apc^{Min/+}$ cells, 9.5 nmol vs 1.8 nmol, respectively, after 90 min of incubation with 40 μM HNE. However, when incubation time was short (5 min), satHNE was higher for $Apc^{Min/+}$ cells. For HNE and DHN glutathione conjugates, the difference between cell types was less important and in favor of preneoplastic cells, especially when the concentration was high (40 μM) and incubation times were long. For HNA and satHNA (peak 33), the difference was in favor of $Apc^{Min/+}$ cells and only for high concentration (40 μM) but low incubation times.

For some biotransformation pathways, namely, cysteine and HNE saturation and/or oxidation, we have performed several complementary experiments in order to identify the enzymes involved.

Radio-HPLC profiles of intracellular unbound metabolites, representing, respectively, 3 and 10% of radioactivity for $Apc^{+/+}$ and $Apc^{Min/+}$ cells after 5 min of 40 μM HNE treatment and 2 and 5% after 30 min treatment, revealed essentially GSH conjugates (results not shown).

Conjugation Pathways. Cysteine conjugation to HNE has been observed by our group and other authors,[24,25] but it is usually lower than GSH conjugation. As incubations with HNE were performed in DMEM, a culture medium that contains a relatively high concentration of cystine, the influence of medium
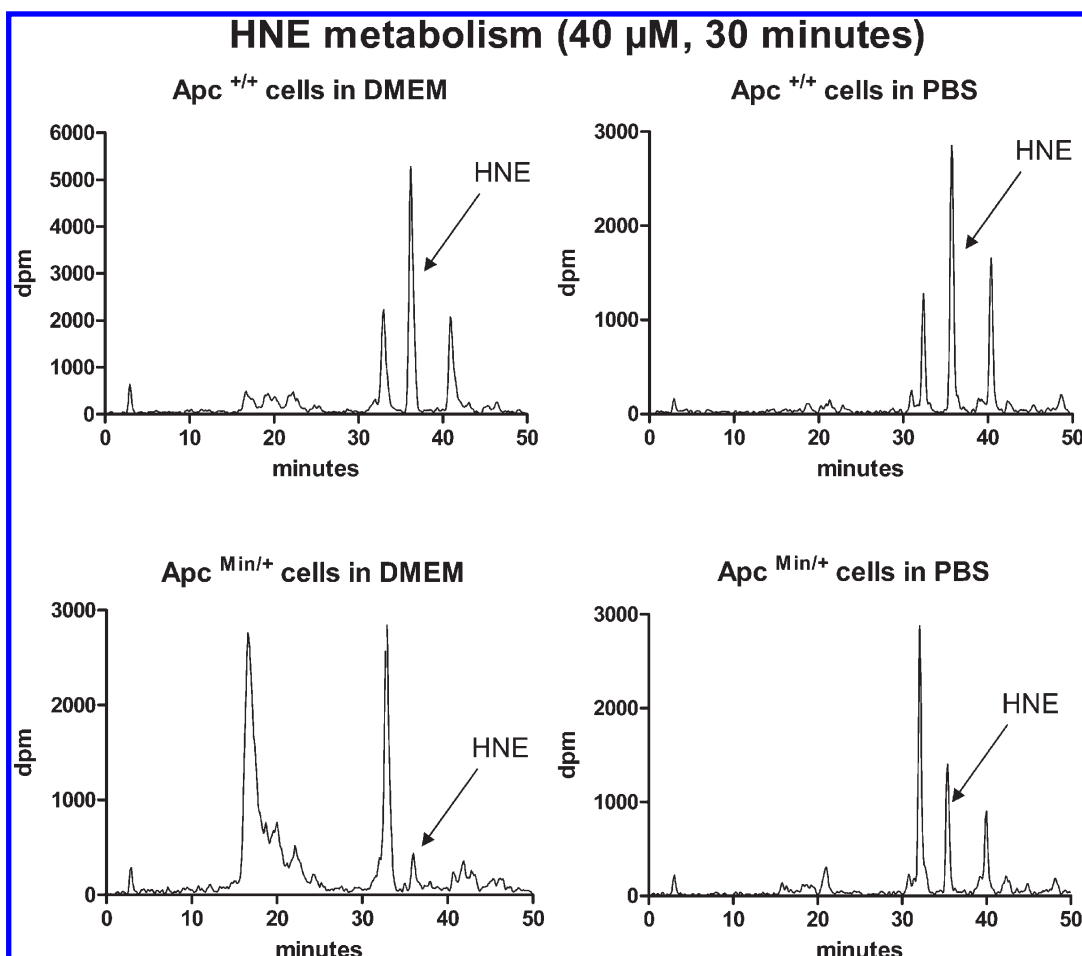
Figure 2. Radio-HPLC profiles of 30 min treatment with 40 μM radiolabeled HNE of Apc$^{+/+}$ cells (top) and of Apc$^{Min/+}$ cells (bottom) in DMEM culture medium (left) or in PBS (right).
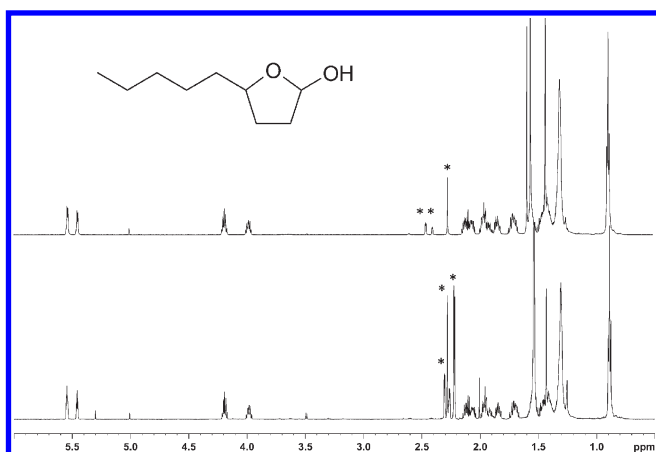

Figure 3. NMR spectra of synthesized 4-hydroxynonanal hemiacetal (satHNE) (top) and of collected Peak 41 (bottom). Sample isolated by HPLC and the standard synthesized were dissolved in 600 μL of deuterated chloroform (CDCl$_3$). Peaks under * are impurities.

composition on HNE−cysteine formation was studied. We performed the same incubations, but we replaced DMEM by PBS buffer, and we observed a dramatic reduction in both GSH and cysteine conjugates (Figure 2). As such, a high cysteine conjugation is likely to occur mainly outside the cell because cells

do not contain high concentrations of cysteine due to its toxicity.[26] Then, we preincubated cells with cystine at the same concentration found in DMEM culture medium (0.2 mM) for 30 min, and we incubated the supernatant with 30 μM HNE for 30 min. As expected, the amount of conjugates was much higher for Apc$^{Min/+}$ cell supernatants, 72% vs 32%, confirming that this conjugation would occur extracellularly.

As cystine must be reduced to give cysteine and because this is likely to occur intracellularly followed by an efflux step that is known to be nonlimiting, we studied the expression of the cystine transport systems in the two cell types. We first performed studies by replacing sodium by lithium in our culture medium to see whether the sodium pump was involved in the difference between cell types. As no difference was observed with this replacement (data not shown), we studied the expression of xCT (SLC7A11), which is a member of the heterodimeric amino acid transport system X$_c^-$, known to be involved in cystine entry in the cell in exchange for glutamate.[27] Quantitative RT-PCR analysis revealed an increased expression of the xCT transcript for preneoplastic cells, with no effect of 40 μM HNE treatment (30 min) (Figure 4). We also analyzed the expression of the enzyme involved in HNE-GSH conjugation, namely, GSTA4-4, and we also observed an increased expression for Apc$^{Min/+}$ cells and no effect of HNE treatment.

HNE Saturation Pathway. SatHNE was quantitatively an important metabolite for Apc$^{+/+}$ cells. It was the major one after a 40 μM HNE treatment, except when the incubation time was

E

dx.doi.org/10.1021/tx2003036 |*Chem. Res. Toxicol.* XXXX, XXX, 000–000

Table 1. HNE Metabolism Studies[a]

| | | (A) As a Function of HNE Concentration (Incubation Time: 30 min) | | | |
| | | retention time | | | |
HNE (μM)	cell type	16.50 (HNE-cysteine)	[17.2; 22] (GSH conjugates)	33.00 (oxidized metabolites)	41.00 (SatHNE)
5	Apc$^{+/+}$	367 ± 121	1072 ± 165	1475 ± 272	702 ± 33
	Apc$^{Min/+}$	1733 ± 333**	896 ± 96	1653 ± 349	283 ± 31***
10	Apc$^{+/+}$	787 ± 136	2105 ± 148	2493 ± 235	1767 ± 172
	Apc$^{Min/+}$	3373 ± 572**	2013 ± 314	3103 ± 766	360 ± 252***
20	Apc$^{+/+}$	1327 ± 506	4113 ± 237	4600 ± 702	3613 ± 528
	Apc$^{Min/+}$	7233 ± 863***	3787 ± 666	5880 ± 1427	687 ± 372***
40	Apc$^{+/+}$	1893 ± 640	5120 ± 1402	6787 ± 1080	8173 ± 1354
	Apc$^{Min/+}$	13813 ± 3698**	7747 ± 201*	9467 ± 522	2833 ± 1040**

| | | (B) As a Function of Incubation Time (HNE Concentration: 40 μM) | | | |
| | | retention time | | | |
time (min)	cell type	16.50 (HNE-cysteine)	[17.2; 22] (GSH conjugates)	33.00 (oxidized metabolites)	41.00 (SatHNE)
5	Apc$^{+/+}$	467 ± 321	1307 ± 583	1640 ± 418	2480 ± 320
	Apc$^{Min/+}$	7467 ± 2854*	3547 ± 1421	3907 ± 760*	3840 ± 382**
10	Apc$^{+/+}$	1760 ± 226	2700 ± 1329	2440 ± 396	4700 ± 707
	Apc$^{Min/+}$	11280 ± 3338**	6080 ± 1867*	6300 ± 424***	4140 ± 1556
30	Apc$^{+/+}$	2107 ± 699	4480 ± 943	6973 ± 1476	8400 ± 1424
	Apc$^{Min/+}$	12987 ± 2560**	8400 ± 773**	9453 ± 189*	2493 ± 1749*
90	Apc$^{+/+}$	3180 ± 674	7320 ± 312	13440 ± 917	9520 ± 629
	Apc$^{Min/+}$	10813 ± 2580**	9573 ± 660**	13653 ± 824	1800 ± 1035***

[a] Radio-HPLC peaks are expressed as picomoles of metabolites. Data are expressed as the mean of three separate experiments ± S.D. *, **, and *** show statistical differences (Student's t test) between Apc$^{+/+}$ and Apc$^{Min/+}$, at $p < 0.05$, $p < 0.01$, and $p < 0.001$, respectively.

long. This result suggested that SatHNE was a primary metabolite that was further biotransformed, probably by oxidation: thus, the peak corresponding to oxidized metabolites was the most important at 90 min after HNE treatment in normal cells (Table 1). To determine the sequence of this putative pathway, we have isolated satHNE/peak 41, which was incubated with the two cell types. HPLC analysis of supernatants gave a peak corresponding to satHNA at Rt = 33 min (Figure 5), whose identification was further confirmed by LC/MS. This peak was much more important after incubations with preneoplastic cells indicating that these cells showed a better oxidative capacity toward this metabolite than normal cells. This could explain the low amount of satHNE observed for the preneoplastic cells in the metabolic profile (Figure 2). The reduction of the α,β-carbon–carbon double bond has been described by Dick et al.[28] for HNE and other α,β-unsaturated aldehydes and ketones. These authors showed that this reaction could be catalyzed by NAD(P)H-dependent alkenal/one oxidoreductase (AO). We have analyzed by quantitative RT-PCR the expression of AO and different aldehyde dehydrogenases (ALDH). We did not observe any difference in the expression of AO between the two cell lines (Figure 4). On the contrary, the expressions of ALDH 1A1, ALDH3A1, and ALDH2 were increased in preneoplastic cells, with no effect of HNE treatment (Figure 4).

Cytotoxicity Assays. As satHNE represented a major metabolite in normal cells, and as those cells were more susceptible to HNE cytotoxicity, synthesized satHNE and satHNA cytotoxicity was tested in both cell types. Both metabolites were not cytotoxic to the two cell types, with treatment concentrations ranging from 5 to 320 μM.

■ DISCUSSION

Although colon adenoma and carcinoma cell lines are well suited to demonstrate the chemoprotective properties of food components or drugs in CRC, those transformed cell lines do not model the physiological targets of promoting agents. Up to now, *in vitro* studies done on the effect of food originating components, and particularly HNE, on CRC development have been performed only on human or mouse colon carcinoma or adenoma cell lines. These transformed cell lines are poorly suited to investigate the biological effect of colon cancer promoters since normal or premalignant epithelial cells are the physiological targets of these components.[29] Hence, mechanistic conclusions for cancer promotion could not really be extrapolated from these *in vitro* studies. In colon carcinogenesis, mutations in the adenomatous polyposis coli (*APC*) gene on the chromosome 5q21 locus are considered to be one of the earliest events in the initiation and promotion of colorectal cancer.[30] *APC* is a tumor suppressor gene. Germline mutation of the *APC* gene determines the familial adenomatous polyposis (FAP) syndrome. Most colorectal cancers are sporadic (90%), but they share with FAP tumors the same early *APC* mutation in 50–80% of cases. In most sporadic colon cancers, like in FAP, a consequence of *APC* gene mutation is ß-catenin accumulation. APC protein controls ß-catenin activity through the canonical Wnt signaling pathway. *APC* mutation provokes the nuclear translocation of ß-catenin and the subsequent activation of c-myc, cyclin D1, and c-jun, involved in cell-cycle regulation.[31] The disruption of the Wnt/ß-catenin pathway is thus a major event in most colon cancers. The consequences of Apc mutation are well-documented, but few

studies have been conducted to explore the direct links between Apc mutation and the relationship of food/colon carcinogenesis. Thus, *in vitro* studies with *Apc*-mutated and nonmutated epithelial cells seem more suitable than carcinoma cell lines for drawing conclusions on the effect of food components in colon cancer promotion. We obtained an intestinal cell line derived from C57BL/6J mice (Apc$^{+/+}$) and Min mice (Apc$^{Min/+}$), which retains the heterozygous Apc genotype and the disordered actin cytoskeleton network for the Apc$^{Min/+}$ cell line.[21,22] This cellular model can contribute to a better understanding of biological effects of promoters on nonmutated (Apc$^{+/+}$) or premalignant cells (Apc$^{Min/+}$). The importance of such cell culture systems modeling different stages of tumorigenesis in the comprehension

of mechanisms by which dietary components impact cancer progression has been described by Fenton et al.[32] In a previous work, we showed that HNE was more cytotoxic to Apc$^{+/+}$ cells than to Apc$^{Min/+}$ cells, at concentrations between 10 and 100 μM. This could be related to the fact that *Apc* mutation has been shown to reduce the level of caspases 3, 7, and 9 in mouse colonocytes, leading to a resistance to apoptosis.[33] However, the present study supports the involvement of a better biotransformation capacity in preneoplastic cells. The concentrations we used (0−40 μM) for HNE treatment of the cells were in the range of what was found in a previous work in the feces of rats fed on diets containing red meat.[15]

Few teams have investigated the impact of Apc mutation on metabolism. In fact, Bellocq et al.[34] investigated the metabolism of the prominent heterocyclic aromatic amine PhIP by the same cellular model, after induction by 2,3,7,8-tetrachlorodibenzo-*p*-dioxin. They described a higher metabolic bioactivation property toward ^{14}C-PhIP for premalignant cells than for normal ones. More recently, the same authors reported again a higher biotransformation activity toward oestradiol-17β for premalignant cells than for Apc$^{+/+}$ cells, even in the absence of dioxin induction.[35] Giera et al.[36] reported an increased expression of glutathione transferases of the μ subfamily correlated to the activation of the Wnt/ß-catenin signaling pathway, a pathway activated by *Apc* mutation (see above).

In the present study, we chose different time and concentration courses within the range in which we previously observed a differential cytotoxicity between the two cell lines, 24 h after HNE treatment. We observed a rather low degradation rate of HNE by our two cell types, with 38% and 6% of unmetabolized HNE after 30 min of incubation, for normal and preneoplastic cells, respectively. In fact, this time course of 40 μM HNE degradation was quite similar to the one very recently reported by Siems et al.[37] for resting or stimulated polymorphonuclear leukocytes treated by 10 μM HNE, with 38% and 13% of remaining HNE after 30 min of incubation, respectively. It was, however, very different from what the same authors observed for other cell types, such as rat hepatocytes or rabbit fibroblasts, for which less than 1% of initial HNE could be found after 3 min of incubation.[37,38] Grune et al.[39] reported a similar HNE utilization between rat enterocytes of the small intestine and hepatocytes, while Esterbauer et al.[40] reported a nearly undetectable HNE-metabolizing activity for the rat small intestine homogenate.
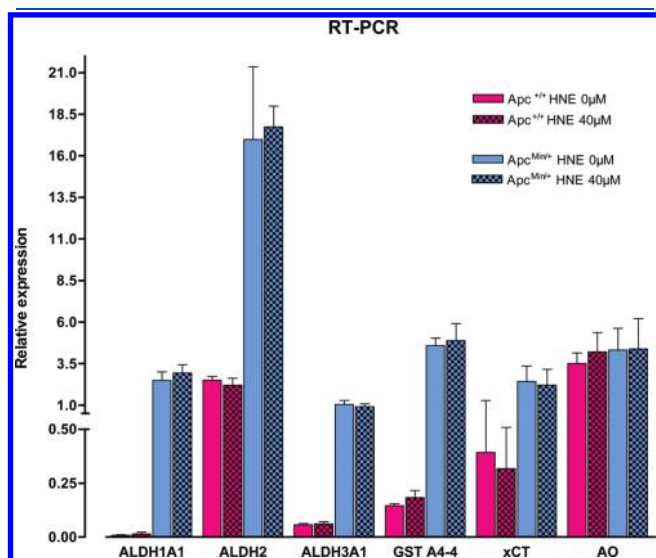

Figure 4. Relative expression of some HNE-related enzymes and transporters between Apc$^{+/+}$ and Apc^{Min+} cells, with or without 40 μM HNE treatment for 30 min, analyzed by quantitative RT-PCR. Data are expressed as the mean of three separate experiments ± SD. Data were analyzed by ANOVA, and means were compared by the Newman−Keuls test. Except for AO for which no statistical difference was observed, all differences between cell lines are statistically significant at $p < 0.001$ except for xCT for which $p < 0.01$. HNE treatment has no statistically significant effect.
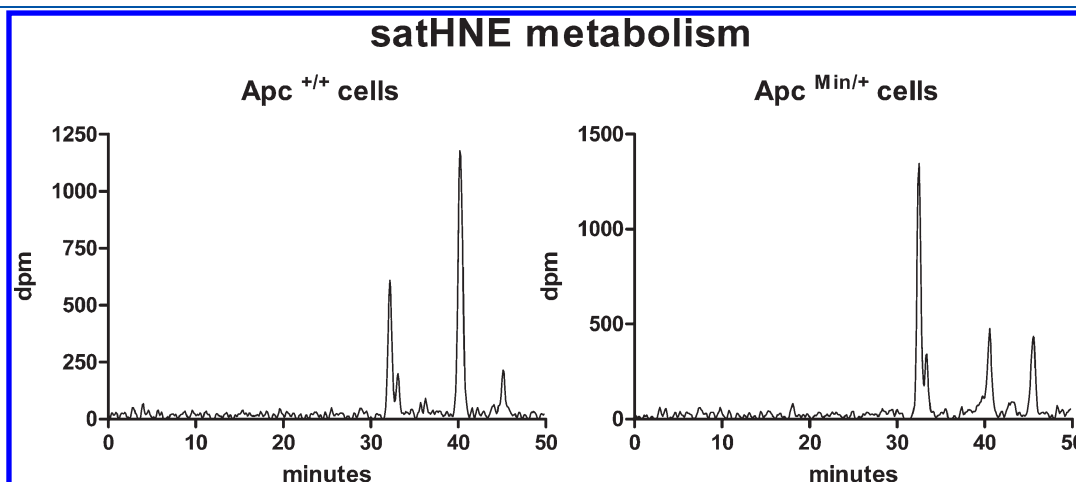

Figure 5. Radio-HPLC profiles of 30 min treatment with collected Peak 41/satHNE of Apc$^{+/+}$ cells (left) and of Apc$^{Min/+}$ cells (right).

We have observed an increased metabolization ability of preneoplastic cells compared to normal cells, which could explain the better resistance of preneoplastic cells toward HNE cytotoxic properties observed in our previous work.[15] This difference can be attributed to a better capacity of using protective thiol-containing cysteine or glutathione to form unreactive conjugated metabolites and to a better capacity to form carboxylated metabolites from the aldehyde function.

The important amount of cysteine conjugates obtained, particularly in preneoplastic cells, is obviously due to the presence of cystine in the culture medium. Cysteine/cystine is a major low-molecular-weight thiol/disulfide redox system in most extracellular fluids. However, the redox potential found in culture medium, with 0.2 mM cystine and no cysteine, is rather oxidizing. CaCo-2 colonic epithelial cells were reported to be able to regulate this oxidizing redox potential to a more physiological one, by the use of sodium-dependent and independent systems that involve the uptake of extracellular cystine, its intracellular reduction, and the efflux of cysteine.[41] Cysteine can then serve as an extracellular trap to scavenge potentially harmful electrophilic compounds, such as HNE, or be used for the de novo synthesis of intracellular GSH, also involved in HNE biotransformation. Those systems involve xCT, the substrate specific subunit of the cystine/glutamate antiporter. We report here that the expression of xCT is increased in preneoplastic cells compared to Apc$^{+/+}$ cells and that could explain the better conjugation capacities for preneoplastic cells. This is in accordance with the fact that this cystine/glutamate antiporter is widely expressed in many cancer cell lines and in primary tumors (for a review see ref 42) including human colon CaCo-2 differentiated or undifferentiated cells.[43] These results are in agreement with a better resistance of those precancerous cells toward oxidative insults.

We report here the presence of 4-hydroxynonanal in its cyclic hemiacetal form (satHNE) as a major metabolite for normal colonocytes. This metabolite has been first evidenced by Dick et al.[28] after treatment by HNE of transfected human kidney embryonic cells with a rat liver NAD(P)H-dependent alkenal/one oxidoreductase (AO) expression vector, an enzyme also known as leukotriene B4 12-hydroxydehydrogenase, 15-oxo-prostaglandin 13-reductase, or dithiolethione-inducible gene-1. This metabolite has not been described in most of the HNE metabolism studies, probably because of its low stability. On the contrary, its oxidized metabolite (satHNA) has been evidenced before in our laboratory in rat precision-cut liver slices[24] and by others in astrocytes, but in its lactone form, namely, γ-nonalactone.[44] In the study in liver slices, the existence of satHNA was attributed to HNA reduction. Our present results indicate that satHNA might likely originate from the oxidation of satHNE. Because of the high formation of satHNE in normal colonocytes, we were able to identify it by means of NMR analysis together with the use of an authentic standard. This primary metabolite is rapidly oxidized in satHNA by preneoplastic cells. Hence, it is difficult to determine whether its formation is higher in normal cells compared to preneoplastic ones, or if the reason of this difference is due to a better secondary oxidative metabolism of this metabolite by preneoplastic colonocytes, as we were not able to resolve the HNA/satHNA peak. The fact that there is no difference between the two cell types in the expression of the AO enzyme and, on the contrary, a huge difference in the one of ALDH1A1 would be an argument for the second explanation. ALDH1A1 is known to have a substrate preference

Scheme 1. Proposed Metabolic Pathways for the Metabolism of HNE in Mouse Colonocytes^a
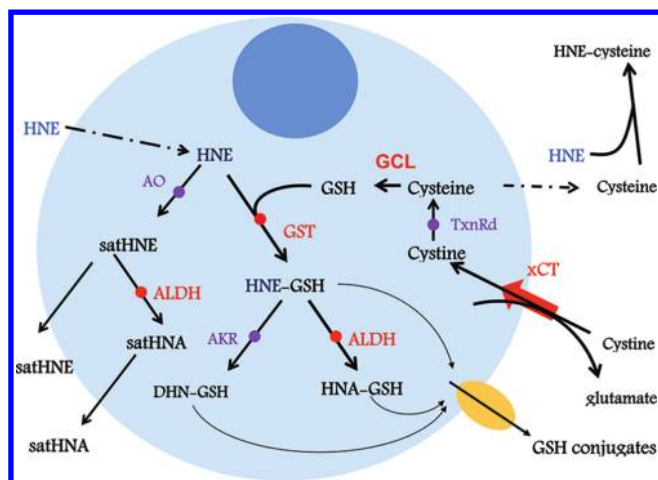
^{a} The red circles and arrow show up-regulated pathways in Apc^{Min+}cells. Purple circles show unchanged pathways in the two cell lines. Orange circle: glutathione conjugate transporter. Blue: extracellular HNE. AKR, aldo-keto reductase; ALDH, aldehyde dehydrogenase; AO, NAD(P)H-dependent alkenal/one oxidoreductase; GCL, glutamate cysteine ligase; GSH, glutathione; GST, glutathione transferase; SatHNA, 4-hydroxy-nonanoic acid; satHNE, 4-hydroxynonanal hemiacetal; TxnRd, thioredoxin reductase; xCT, member of the heterodimeric amino acid transport system x_{c-}.

for aldehydic lipid oxidation products such as HNE and malondialdehyde.[45]

Our results show that some pathways involved directly (such as glutathione conjugation and HNE oxidation) or indirectly in HNE biotransformation (such as cystine uptake) are upregulated in preneoplastic cells when compared to normal ones (Scheme 1). To our knowledge, there is no direct link between the regulation of the expression of such enzymes and the Apc/Wnt pathway. The only known study concerned GSTs of the μ subfamily,[36] but HNE metabolism preferentially involves GSTs from the α subfamily, particularly GSTA4-4.[46] However, some of the enzymes probably involved in those metabolism pathways share a common induction by the nuclear erythroid related factor 2/antioxidant responsive element (Nrf2/ARE) pathway, a pathway that regulates the expression of many mammalian detoxification and antioxidant enzymes under conditions of oxidative or electrophilic stress.[47] GSTA4-4, a GST specific for HNE conjugation to GSH and γ-glutamylcysteine synthetase, the rate-limiting enzyme for GSH synthesis, were reported to be regulated by this pathway.[48,49] Nrf2 activators were reported as inducers of ALDH1A1 expression.[45] The substrate specific subunit of the cystine/glutamate antiporter xCT is also under the regulation of this pathway.[50] Apc-mutated cells would be programmed to resist to HNE treatment, through the up-regulation of HNE metabolizing genes and possibly through a permanent activation of Nrf2. This is in accordance with the previous reports that describe a permanent activation of Nrf2 observed in some cancerous cells, either by inactivation of the Nrf2 repressor Kelch-like ECH-associated protein 1 (Keap1) observed in different tumor types (but not CRC) or by a direct mutation of Nrf2, evading Keap1 repression[51] leading to increased Nrf2 translocation into the nucleus and subsequent upregulation of ARE-dependent cytoprotective genes. HNE itself is known to activate this pathway and to induce the expression of xCT in cardiomyocytes.[52]

However, in the present study, we did not observe any effect of HNE treatment on the expression of the different tested enzymes. This could be due to the short treatment time we used (30 min) in relation to HNE-metabolizing activities. Further work will provide new data about the role of Nrf2 in *Apc*-mutated cells.

Apc mutation induces in cells a better capacity to get rid of potentially harmful dietary secondary lipid oxidation products through coordinated biotransformation pathways and a subsequent survival advantage for the mutated cells in a peroxidative environment. Such an environment is likely to be found in the colon lumen, when the diet is rich in heme iron but poor in counterbalancing compounds, such as antioxidants or heme-chelating agents. These new results could provide a relevant explanation of the epidemiologic relationship between red and processed meat intake and colorectal cancer risk.

■ AUTHOR INFORMATION

Corresponding Author
*Tel: 00-33-561-28-50-05.Fax: 00-33-561-28-52-44. E-mail: fgueraud@toulouse.inra.fr.

Funding Sources

■ DEDICATION

This work is dedicated to the memory of Dr. Jacques Alary, our colleague and friend, who started HNE metabolism studies in our group.

■ ABBREVIATIONS

ACF, aberrant crypt foci; ALDH, aldehyde dehydrogenase; AO, NAD(P)H-dependent alkenal/one oxidoreductase; Apc, adenomatous polyposis coli; BHT, 2,6-dibutyl-4-hydroxy-toluene; BSTFA, N,O-bis-trimethylsilyl-trifluoroacetamide; CRC, colorectal cancer; DCM, dichloromethane; DHN, 1,4-dihydroxy-2(E)-nonene; DIBAL, diisobutylaluminium hydride; DMEM, Dulbecco's-modified essential medium; FAP, familial adenomatous polyposis; GST, glutathione transferase; HNA, 4-hydroxy-2(E)-nonenoic acid; HNE, 4-hydroxy-2(E)-nonenal; satHNA, 4-hydroxynonanoic acid; satHNE, 4-hydroxynonanal hemiacetal; TMCS, trimethylchlorosilane; xCT, member of the heterodimeric amino acid transport system X_c^-.

■ REFERENCES

(1) Larsson, S. C., and Wolk, A. (2006) Meat consumption and risk of colorectal cancer: a meta-analysis of prospective studies. *Int. J. Cancer* 119 (11), 2657–2664.

(2) Norat, T., Lukanova, A., Ferrari, P., and Riboli, E. (2002) Meat consumption and colorectal cancer risk: dose-response meta-analysis of epidemiological studies. *Int. J. Cancer* 98 (2), 241–256.

(3) Bastide, N. M., Pierre, F. H., and Corpet, D. E. (2011) Heme iron from meat and risk of colorectal cancer: a meta-analysis and a review of the mechanisms involved. *Cancer Prev. Res. 4* (2), 177–184.

(4) WCRF (2007) *Food, Nutrition, Physical Activity, and the Prevention of Cancer: A Global Perspective*, WCRF and American Institute for Cancer Research, Washington, D.C.

(5) Pierre, F., Freeman, A., Tache, S., Van der Meer, R., and Corpet, D. E. (2004) Beef meat and blood sausage promote the formation of azoxymethane-induced mucin-depleted foci and aberrant crypt foci in rat colons. *J. Nutr. 134* (10), 2711–2716.

(6) Pierre, F., Tache, S., Petit, C. R., Van der Meer, R., and Corpet, D. E. (2003) Meat and cancer: haemoglobin and haemin in a low-calcium diet promote colorectal carcinogenesis at the aberrant crypt stage in rats. *Carcinogenesis 24* (10), 1683–1690.

(7) Santarelli, R. L., Vendeuvre, J. L., Naud, N., Tache, S., Gueraud, F., Viau, M., Genot, C., Corpet, D. E., and Pierre, F. H. (2010) Meat processing and colon carcinogenesis: cooked, nitrite-treated, and oxidized high-heme cured meat promotes mucin-depleted foci in rats. *Cancer Prev. Res. 3* (7), 852–864.

(8) Pierre, F. H., Santarelli, R. L., Allam, O., Tache, S., Naud, N., Gueraud, F., and Corpet, D. E. (2010) Freeze-dried ham promotes azoxymethane-induced mucin-depleted foci and aberrant crypt foci in rat colon. *Nutr. Cancer 62* (5), 567–573.

(9) Sawa, T., Akaike, T., Kida, K., Fukushima, Y., Takagi, K., and Maeda, H. (1998) Lipid peroxyl radicals from oxidized oils and heme-iron: implication of a high-fat diet in colon carcinogenesis. *Cancer Epidemiol. Biomarkers Prev. 7* (11), 1007–1012.

(10) Sesink, A. L., Termont, D. S., Kleibeuker, J. H., and Van der Meer, R. (1999) Red meat and colon cancer: the cytotoxic and hyperproliferative effects of dietary heme. *Cancer Res. 59* (22), 5704–5709.

(11) Esterbauer, H., Schaur, R. J., and Zollner, H. (1991) Chemistry and biochemistry of 4-hydroxynonenal, malonaldehyde and related aldehydes. *Free Radical Biol. Med. 11* (1), 81–128.

(12) Forman, H. J. (2010) Reactive oxygen species and alpha,beta-unsaturated aldehydes as second messengers in signal transduction. *Ann. N.Y. Acad. Sci. 1203*, 35–44.

(13) Gasc, N., Tache, S., Rathahao, E., Bertrand-Michel, J., Roques, V., and Gueraud, F. (2007) 4-hydroxynonenal in foodstuffs: heme concentration, fatty acid composition and freeze-drying are determining factors. *Redox Rep. 12* (1), 40–44.

(14) Gueraud, F., Atalay, M., Bresgen, N., Cipak, A., Eckl, P. M., Huc, L., Jouanin, I., Siems, W., and Uchida, K. (2010) Chemistry and biochemistry of lipid peroxidation products. *Free Radical Res. 44* (10), 1098–1124.

(15) Pierre, F., Tache, S., Gueraud, F., Rerole, A. L., Jourdan, M. L., and Petit, C. (2007) Apc mutation induces resistance of colonic cells to lipoperoxide-triggered apoptosis induced by faecal water from haem-fed rats. *Carcinogenesis 28* (2), 321–327.

(16) Corpet, D. E., Tache, S., and Peiffer, G. (1997) Colon tumor promotion: is it a selective process? Effects of cholate, phytate, and food restriction in rats on proliferation and apoptosis in normal and aberrant crypts. *Cancer Lett. 114* (1−2), 135–138.

(17) Jouanin, I., Sreevani, V., Rathahao, E., Gueraud, F., and Paris, A. (2008) Synthesis of the lipid peroxidation product 4-hydroxy-2(E)-nonenal with C-13 stable isotope incorporation. *J. Label. Compd. Radiopharm. 51* (1−2), 87–92.

(18) Tanikaga, R., Nozaki, Y., Tamura, T., and Kaji, A. (1983) Facile synthesis of 4-hydroxy-(E)-2-alkenoic esters from aldehydes. *Synthesis 2*, 134–135.

(19) Long, E. K., Smoliakova, I., Honzatko, A., and Picklo, M. J. S. (2008) Structural characterization of α,β-unsaturated aldehydes by GC/MS is dependent upon ionization method. *Lipids 43* (8), 765–774.

(20) Bravais, F., Rao, D., Alary, J., Rao, R. C., Debrauwer, L., and Bories, G. (1995) Synthesis of 4-hydroxy[4-H-3]-2(E)-nonen-1-Al-diethylacetal. *J. Label. Compd. Radiopharm. 36* (5), 471–477.

(21) Forest, V., Clement, M., Pierre, F., Meflah, K., and Menanteau, J. (2003) Butyrate restores motile function and actin cytoskeletal network integrity in apc mutated mouse colon epithelial cells. *Nutr. Cancer 45* (1), 84–92.

(22) Pierre, F. (1999) Immunoprophylaxie des cancers colorectaux par des glucides indigestibles fermentables: études chez la souris Min, University of Nantes, Nantes, France.

(23) Jouanin, I., Baradat, M., Gieules, M., Taché, S., Pierre, F. H. F., Guéraud, F., and Debrauwer, L. (2011) LC/ESIMS tracking of 4-hydroxy-2(E)-nonenal biotransformations by mouse colon epithelial cells using [1,2-$^{13}C_2$]-4-hydroxy-2(E)-nonenal as stable isotope tracer. *Rapid Commun. Mass Spectrom. 25*, 2675–2681.

(24) Laurent, A., Perdu-Durand, E., Alary, J., Debrauwer, L., and Cravedi, J. P. (2000) Metabolism of 4-hydroxynonenal, a cytotoxic product of lipid peroxidation, in rat precision-cut liver slices. *Toxicol. Lett.* 114 (1−3), 203–214.

(25) Siems, W., and Grune, T. (2003) Intracellular metabolism of 4-hydroxynonenal. *Mol. Aspects Med.* 24 (4−5), 167–175.

(26) Wang, X. F., and Cynader, M. S. (2001) Pyruvate released by astrocytes protects neurons from copper-catalyzed cysteine neurotoxicity. *J. Neurosci.* 21 (10), 3322–3331.

(27) Huang, Y., Dai, Z., Barbacioru, C., and Sadee, W. (2005) Cystine-glutamate transporter SLC7A11 in cancer chemosensitivity and chemoresistance. *Cancer Res.* 65 (16), 7446–7454.

(28) Dick, R. A., Kwak, M. K., Sutter, T. R., and Kensler, T. W. (2001) Antioxidative function and substrate specificity of NAD(P)H-dependent alkenal/one oxidoreductase. A new role for leukotriene B4 12-hydroxydehydrogenase/15-oxoprostaglandin 13-reductase. *J. Biol. Chem.* 276 (44), 40803–40810.

(29) Marian, B. (2002) In vitro models for the identification and characterization of tumor-promoting and protective factors for colon carcinogenesis. *Food Chem. Toxicol.* 40 (8), 1099–1104.

(30) Narayan, S., and Roy, D. (2003) Role of APC and DNA mismatch repair genes in the development of colorectal cancers. *Mol. Cancer* 2, 41.

(31) Clevers, H. (2004) Wnt breakers in colon cancer. *Cancer Cell* 5 (1), 5–6.

(32) Fenton, J. I., and Hord, N. G. (2006) Stage matters: choosing relevant model systems to address hypotheses in diet and cancer chemoprevention research. *Carcinogenesis* 27 (5), 893–902.

(33) Chen, T., Yang, I., Irby, R., Shain, K. H., Wang, H. G., Quackenbush, J., Coppola, D., Cheng, J. Q., and Yeatman, T. J. (2003) Regulation of caspase expression and apoptosis by adenomatous polyposis coli. *Cancer Res.* 63 (15), 4368–4374.

(34) Bellocq, D., Molina, J., Rathahao, E., Canlet, C., Tache, S., Martin, P. G., Pierre, F., and Paris, A. (2008) High potency of bioactivation of 2-amino-1-methyl-6-phenylimidazo[4,5-b]pyridine (PhIP) in mouse colon epithelial cells with Apc(Min) mutation. *Mutat. Res.* 653 (1−2), 34–43.

(35) Bellocq, D., Molina, J., Rathahao-Paris, E., Tache, S., Pierre, F., and Paris, A. (2010) Metabolic bioactivation of oestradiol-17beta (E2beta) in mouse colon epithelial cells bearing ApcMin mutation. *Steroids* 75 (10), 665–675.

(36) Giera, S., Braeuning, A., Kohle, C., Bursch, W., Metzger, U., Buchmann, A., and Schwarz, M. (2010) Wnt/beta-catenin signaling activates and determines hepatic zonal expression of glutathione S-transferases in mouse liver. *Toxicol. Sci.* 115 (1), 22–33.

(37) Siems, W., Crifo, C., Capuozzo, E., Uchida, K., Grune, T., and Salerno, C. (2010) Metabolism of 4-hydroxy-2-nonenal in human polymorphonuclear leukocytes. *Arch. Biochem. Biophys.* 503 (2), 248–252.

(38) Siems, W. G., Zollner, H., Grune, T., and Esterbauer, H. (1997) Metabolic fate of 4-hydroxynonenal in hepatocytes: 1,4-dihydroxynonene is not the main product. *J. Lipid Res.* 38 (3), 612–622.

(39) Grune, T., Siems, W., Kowalewski, J., Zollner, H., and Esterbauer, H. (1991) Identification of metabolic pathways of the lipid peroxidation product 4-hydroxynonenal by enterocytes of rat small intestine. *Biochem. Int.* 25 (5), 963–971.

(40) Esterbauer, H., Zollner, H., and Lang, J. (1985) Metabolism of the lipid peroxidation product 4-hydroxynonenal by isolated hepatocytes and by liver cytosolic fractions. *Biochem. J.* 228 (2), 363–373.

(41) Mannery, Y. O., Ziegler, T. R., Hao, L., Shyntum, Y., and Jones, D. P. (2010) Characterization of apical and basal thiol-disulfide redox regulation in human colonic epithelial cells. *Am. J. Physiol. Gastrointest. Liver Physiol.* 299 (2), G523–530.

(42) Lo, M., Wang, Y. Z., and Gout, P. W. (2008) The x(c)- cystine/glutamate antiporter: a potential target for therapy of cancer and other diseases. *J. Cell. Physiol.* 215 (3), 593–602.

(43) Bassi, M. T., Gasol, E., Manzoni, M., Pineda, M., Riboni, M., Martin, R., Zorzano, A., Borsani, G., and Palacin, M. (2001) Identification and characterisation of human xCT that co-expresses, with 4F2 heavy chain, the amino acid transport activity system xc. *Pflugers Arch.* 442 (2), 286–296.

(44) Kubatova, A., Murphy, T. C., Combs, C., and Picklo, M. J., Sr. (2006) Astrocytic biotransformation of trans-4-hydroxy-2-nonenal is dose-dependent. *Chem. Res. Toxicol.* 19 (6), 844–851.

(45) Alnouti, Y., and Klaassen, C. D. (2008) Tissue distribution, ontogeny, and regulation of aldehyde dehydrogenase (Aldh) enzymes mRNA by prototypical microsomal enzyme inducers in mice. *Toxicol. Sci.* 101 (1), 51–64.

(46) Hubatsch, I., Ridderstrom, M., and Mannervik, B. (1998) Human glutathione transferase A4−4: an alpha class enzyme with high catalytic efficiency in the conjugation of 4-hydroxynonenal and other genotoxic products of lipid peroxidation. *Biochem. J.* 330 (Pt 1), 175–179.

(47) Itoh, K., Chiba, T., Takahashi, S., Ishii, T., Igarashi, K., Katoh, Y., Oyake, T., Hayashi, N., Satoh, K., Hatayama, I., Yamamoto, M., and Nabeshima, Y. (1997) An Nrf2/small Maf heterodimer mediates the induction of phase II detoxifying enzyme genes through antioxidant response elements. *Biochem. Biophys. Res. Commun.* 236 (2), 313–322.

(48) Hu, R., Xu, C., Shen, G., Jain, M. R., Khor, T. O., Gopalkrishnan, A., Lin, W., Reddy, B., Chan, J. Y., and Kong, A. N. (2006) Gene expression profiles induced by cancer chemopreventive isothiocyanate sulforaphane in the liver of C57BL/6J mice and C57BL/6J/Nrf2 (−/−) mice. *Cancer Lett.* 243 (2), 170–192.

(49) Wild, A. C., Moinova, H. R., and Mulcahy, R. T. (1999) Regulation of gamma-glutamylcysteine synthetase subunit gene expression by the transcription factor Nrf2. *J. Biol. Chem.* 274 (47), 33627–33636.

(50) Sasaki, H., Sato, H., Kuriyama-Matsumura, K., Sato, K., Maebara, K., Wang, H., Tamba, M., Itoh, K., Yamamoto, M., and Bannai, S. (2002) Electrophile response element-mediated induction of the cystine/glutamate exchange transporter gene expression. *J. Biol. Chem.* 277 (47), 44765–44771.

(51) Hayes, J. D., and McMahon, M. (2009) NRF2 and KEAP1 mutations: permanent activation of an adaptive response in cancer. *Trends Biochem. Sci.* 34 (4), 176–188.

(52) Zhang, Y., Sano, M., Shinmura, K., Tamaki, K., Katsumata, Y., Matsuhashi, T., Morizane, S., Ito, H., Hishiki, T., Endo, J., Zhou, H., Yuasa, S., Kaneda, R., Suematsu, M., and Fukuda, K. (2010) 4-hydroxy-2-nonenal protects against cardiac ischemia-reperfusion injury via the Nrf2-dependent pathway. *J. Mol. Cell. Cardiol.* 49 (4), 576–586.